International Journal of Power Electronics and Drive System (IJPEDS)
Vol. 17, No. 2, June 2026, pp. 894~907
ISSN: 2088-8694, DOI: 10.11591/ijpeds.v17.i2.pp894-907

Real-time implementation and comparative analysis of fault-tolerant control strategies for induction motor drives

Asmaa Hammou, Mokhtar Bendjebbar, Mohammed Benslimane
Department of Electrotechnics, Faculty of Electrical Engineering, University of Sciences and Technology of Oran Mohamed Boudiaf, Oran, Algeria

Article Info

Article history:

Received Sep 14, 2025
Revised Dec 19, 2025
Accepted Feb 21, 2026

Keywords:

Direct torque control DTC
DS1104
Fault-tolerant control
Indirect field-oriented control
Induction motor

ABSTRACT

For nearly five decades, the induction motor has been the most widely used electrical machine in industry due to its robustness, simplicity, and low cost, supported by advances in power electronics enabling effective performance control. While DC motors were previously favored for their ease of speed and torque regulation, induction motors have gained prominence because they do not require brushes and involve fewer wear-prone components, resulting in reduced maintenance and improved reliability. Consequently, they are widely employed in industrial applications and emerging fields such as electric and hybrid vehicles. This study presents a comparative analysis of two fault-tolerant control (FTC) strategies: field-oriented control (FOC) and direct torque control (DTC). The evaluation focuses on sensitivity to parameter variations, dynamic performance, and steady-state behavior. Both strategies, classified under vector control techniques, are implemented in real time using a dSPACE platform to control an induction motor under an open-circuit fault in a two-level inverter. Results demonstrate that the DTC-based FTC approach offers superior robustness and stability compared to the IFOC-based method, particularly under fault conditions, load disturbances, and speed variations.

Corresponding Author:

Mokhtar Bendjebbar
Department of Electrotechnics, Faculty of Electrical Engineering
University of Sciences and Technology of Oran Mohamed Boudiaf
El Mnaouar, Bp 1505, Bir El Djir 31000, Oran, Algeria
Email: mokhtar.bendjebbar@univ-usto.dz

1. INTRODUCTION

Induction motor drives are extensively employed in a wide range of industrial applications owing to their superior steady-state performance and rapid dynamic response. The growing demand for safety, reliability, and service continuity in industrial processes has prompted significant research efforts in fault detection and diagnosis, and more recently, in the development of fault-tolerant control systems [1]. For example, when a machine exhibits an open-phase fault, this results in current harmonics, torque ripples, reduced maximum applicable voltage, and limitations on the achievable base speed for permanent magnet synchronous motors and three-phase induction motors.

Several authors have proposed applying robust fault-tolerant control techniques, such as sliding mode control or DTC-based approaches. They concluded that these techniques deliver remarkable and comparable performance, while also offering improved stability. These methods are classified as passive approaches [2], [3]. Passive approaches rely on robust control capable of maintaining acceptable performance without requiring a diagnostic block or controller reconfiguration. Active approaches, however, require a

fault detection and isolation (FDI) block, along with a control reconfiguration strategy based on information provided by the diagnostic block [4], [5].

The application of induction motors in traction systems, particularly in electric vehicles, requires a comparative analysis of available traction drive strategies. Among the most widely used are indirect field-oriented control (IFOC) and direct torque control (DTC), both functioning as torque control techniques. IFOC, introduced in the 1970s, operates without the need for flux estimation, whereas DTC, developed in the mid-1980s [6], [7], relies on flux estimation.

Both approaches exhibit similar characteristics, including the regulation of torque and flux, rapid torque response, and sensitivity to variations in motor parameters. In conventional IFOC, flux control is associated with the rotor flux aligned along the d-axis in the synchronous reference frame. In contrast, DTC regulates the stator flux within the same reference frame. The comparison between these control methods is often based on their respective switching strategies. IFOC employs independent control of electromagnetic torque and rotor flux (as illustrated in Figure 1), while DTC utilizes a switching table to maintain electromagnetic torque and stator flux within predefined hysteresis bands (see Figure 2).

This study examines the dynamic performance of both IFOC and DTC under low-frequency speed control conditions. It also evaluates their sensitivity to inaccuracies in motor parameters. For IFOC, critical parameters include magnetizing inductance, rotor resistance, and rotor inductance, whereas in DTC, stator resistance is particularly significant. Two types of induction motor control schemes are analyzed—both in terms of dynamic and steady-state performance through simulation and experimental implementation. Recommendations for their application are provided, based on the mathematical principles underlying each controller, and the results obtained from the two control algorithms analyzed are DTC and IFOC. Simulations for each control type are performed in MATLAB/Simulink to study the sensitivity to internal machine parameters, and real-time implementations using a dSPACE 1104 board are conducted for comparison.

To the best of our knowledge, no direct comparisons of the dynamic responses of IFOC and DTC have been reported in the literature. Existing studies on parameter sensitivity do not quantify the impact of parameter variations or errors on transient responses. Most publications focus primarily on steady-state performance [8]-[11], while [11], [12] offer only limited comparisons of dynamic behavior.

In contrast, the study in [13] proposes a type-2 fuzzy logic controller aimed at enhancing the performance of the conventional PI controller within the indirect field-oriented control (IFOC) strategy under broken-bar conditions. The authors report that this approach also improves robustness against motor parameter variations. Similarly, the work in [14] presents a robust, sensorless fault-tolerant controller for induction motors, employing a backstepping strategy to compensate for load-torque disturbances and rotor-resistance variations resulting from broken rotor bars.

The results indicate that the machine sustains acceptable performance even after fault occurrence. The proposed method does not require a diagnostic module or controller reconfiguration and is therefore classified as a passive fault-tolerant approach, making it suitable for safety-critical applications until final maintenance can be performed. The increasing demand for reliability and safety in industrial systems exposed to process anomalies and component failures makes early detection and identification of faults essential. Fault-tolerant operation is required to minimize performance degradation and prevent hazardous conditions. Over recent decades, various fault-diagnosis techniques have been proposed, which can be broadly categorized into three groups: hardware-redundancy approaches, signal-based approaches, and model-based analytical approaches [15].

As presented in [16], fault-tolerant inverter topologies often rely on hardware redundancy when a converter leg becomes unavailable. A similar concept was adopted in [17] for phase-loss tolerance in traction-oriented induction motors, using a dual-inverter reconfiguration strategy. Gate-drive open-circuit faults can arise from bond-wire lift-off caused by thermal cycling, driver malfunctions, or IGBT rupture triggered by short-circuit conditions. These faults induce DC current offsets in both the affected and healthy phases. The interaction between the DC component and the magnetic field generates torque pulsations at the stator-current frequency, markedly reducing the maximum average torque available for traction [18].

These DC offsets also induce uneven stress on the inverter switches, potentially causing secondary failures in the converter, the motor, or the load. Since voltages and currents carry distinguishable fault signatures, they can be analyzed for fault detection and localization. Although open-circuit faults do not generally lead to immediate shutdown, they degrade system performance; hence, their diagnosis is essential in fault-tolerant converter systems [19].

In model-based diagnostic approaches, fault detection relies on a mathematical model operating in parallel with the real system. Diagnostic variables are obtained by comparing the actual system outputs with those predicted by the model. In this context, the study in [20] proposes a nonlinear observer for estimating rotor fluxes and stator currents in the (d, q) rotating frame. Open-circuit insulated gate bipolar transistor (IGBT) faults are detected by evaluating the residuals between measured and estimated stator currents. This method is load-independent and requires no additional circuitry.

Similarly, Chikondra *et al.* [21] present a fault-tolerant control scheme for a five-phase induction motor supplied by a three-level NPC VSI, based on direct torque control (DTC) principles. The strategy guarantees continuous operation even in the event of an open-phase fault. A significant advantage is that the controller requires no reconfiguration upon fault occurrence, making it a promising option for integration into fault-tolerant drive architectures.

To incorporate efficiency, thermal considerations, and long-term reliability requirements in safety-critical real-time systems, it is necessary to accurately monitor component performance, lifetime, and cost. Fault tolerance inherently involves a trade-off between performance and reliability. Long-duration, high-performance processes often employ checkpoint and rollback mechanisms to achieve fault tolerance, as they reduce overall program execution time after a failure. Checkpointing remains a relatively cost-effective technique [22].

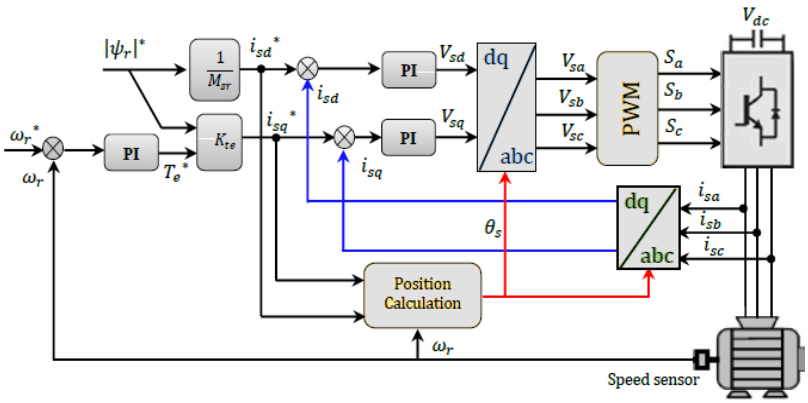

Figure 1. IFOC Block diagram

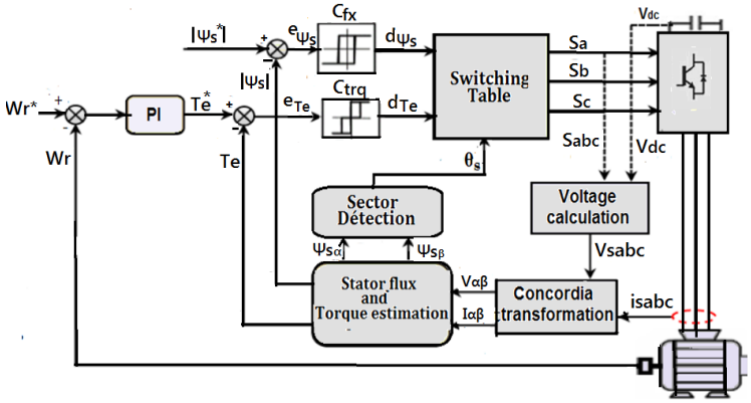

Figure 2. DTC block diagram

2. INDUCTION MACHINE MODEL

The model used for the induction machine is established in a reference frame aligned with the rotating magnetic field (generally the synchronized dq reference frame). Within this framework, the stator currents, rotor fluxes, and electromechanical speed are considered state variables, while the stator voltages are treated as control variables.

This dynamic model can be expressed using (1)-(6):

$$\frac{d}{dt}I_{sd} = -\lambda I_{sd} + \omega_s I_{sq} + \frac{k_s}{T_r}\psi_{rd} + k_s\omega_r\psi_{rq} + \frac{1}{\sigma L_s}V_{sd} \quad (1)$$

$$\frac{d}{dt}I_{sq} = -\omega_s I_{sd} - \lambda I_{sq} + \omega_r k_s\psi_{rd} + \frac{k_s}{T_r}\psi_{rq} + \frac{1}{\sigma L_s}V_{sq} \quad (2)$$

$$\frac{d}{dt}\psi_{rd} = \frac{M}{T_r} I_{sd} - \frac{1}{T_r}\psi_{rd} + (\omega_s - \omega_r)\psi_{rq} \quad (3)$$

$$\frac{d}{dt}\psi_{rq} = \frac{M}{T_r} I_{sq} - (\omega_s - \omega_r)\psi_{rd} - \frac{1}{T_r}\psi_{rq} \quad (4)$$

$$T_e = p\frac{M}{L_r}(\psi_{rd} I_{sq} - \psi_{rq} I_{sd}) \quad (5)$$

$$\frac{d}{dt}\Omega_r = \frac{1}{J}(T_{em} - T_r) - \frac{f}{J}\Omega_r \quad (6)$$

with:

$$\lambda = \frac{R_s}{\sigma L_s} + \frac{R_r M^2}{\sigma L_s L_r^2} \; : \; k_s = \frac{M}{\sigma L_s L_r} \; ; T_r = \frac{L_r}{R_r} \; ; \; \sigma = 1 - \frac{M^2}{L_s L_r}$$

where I_{sq}, I_{sd}: (d,q) stator currents, ψ_{rd}, ψ_{rq}: (d,q) rotor fluxes, V_{sd}, V_{sq}: (d,q) stator voltages, ω_s, ω_r: synchronous speed-angular speed, Ω_r: mechanical rotational speed, and T_e, T_r: electromagnetic torque-resistant torque.

3. ROTOR FLUX ORIENTED CONTROL

The rotor flux-oriented control of an induction motor aims to make the machine's behavior analogous to that of a separately excited DC motor, in which the flux and torque controls are independent. To achieve this, the control reference frame is oriented such that:

$$\psi_{rd} = \psi_r \quad and \; \psi_{rd} = 0 \quad (7)$$

Aligning the rotor flux vector with the d-axis greatly simplifies the model, with *B* as a constant matrix and A as a nonlinear matrix. Substituting in (7) into the model equations (notably in (3) and (5), we obtain the following expressions:

- Rotor flux

$$\psi_r = \frac{M}{T_r s + 1} I_{sd} \quad (8)$$

- Electromagnetic torque

$$Te = p\frac{M}{L_r}\psi_r I_{sq} \quad (9)$$

In this configuration, the torque depends only on the stator currentI_{sq} in (10), which makes the behavior very similar to that of a DC motor:

$$Te = \mathrm{k}'.\psi_r.I \quad (10)$$

where ϕ_{is} the flux and I_{is} the armature current (here I_{sq}). Thus, two independent control variables are distinguished: $I_{sd}\rightarrow$ to regulate the flux and $I_{sq}\rightarrow$ to control the torque.

- Rotating field position (angular speed)

In this context, in (4) becomes:

$$\omega_s = \frac{M}{T_r \psi_r} I_{sq} + p\Omega_r \quad (11)$$

and the stator angle used in all abc ↔ dqo transformations is obtained by integration:

$$\theta_s = \int \omega_s dt \quad (12)$$

The overall diagram of the IRFOC scheme of an IM is illustrated in Figure 1.

4. FAULTY MATHEMATICAL MODEL OF IM AND PROBLEM FORMULATION

The dynamic model of an induction motor (IM) in the stator reference frame can be described as (13) and (14).

$$\dot{x} = Ax + Bu \tag{13}$$

$$\begin{cases} x = [x_1 x_2 x_3 x_4]^T = [i_{s\alpha} i_{s\beta} \psi_{r\alpha} \psi_{r\beta}]^T \\ u = [u_1 u_2]^T = [v_{s\alpha} v_{s\beta}]^T \end{cases} \tag{14}$$

Consider the induction motor model described by (13), which is subject to faults that may be electrical in nature, as discussed in [23].

$$\dot{x} = Ax + Bu + D_f F \tag{15}$$

In the absence of faults, F is identically zero, and it follows that (16).

$$\begin{cases} D_f = \begin{bmatrix} 1 & 0 & 0 & 0 \\ 0 & 1 & 0 & 0 \end{bmatrix}^T \\ F = [F_1 F_2]^T \end{cases} \tag{16}$$

Electrical and/or mechanical faults introduce asymmetries in the induction motor (IM), leading to the generation of slot harmonics in the stator windings (17).

$$\begin{cases} x_1 \rightarrow x_1 + F_{h1} \\ x_2 \rightarrow x_2 + F_{h2} \end{cases} \tag{17}$$

Where:

$$\begin{cases} F_{h1} = \sum_i^{n_f} A_i \sin(\omega_i t + \varphi_i) \\ F_{h2} = \sum_i^{n_f} A_i \cos(\omega_i t + \varphi_i) \\ \omega_i = 2\pi f_i + 2\pi f_a = 2\pi (f_i + f_a) \end{cases} \tag{18}$$

with: n_f: number of faults, f_i: characteristic fault frequency, and f_a: fundamental frequency.

5. DIRECT TORQUE CONTROL (DTC) [24]

DTC is a control strategy in which the motor torque and speed are directly regulated based on its electromagnetic state, similarly to a direct current (DC) motor. Unlike conventional Pulse Width Modulation (PWM) methods, which adjust the input voltage and frequency, DTC enables direct control of key physical variables such as torque and flux. For induction motors (IM), the conventional DTC principle relies on the direct selection of stator voltage vectors using hysteresis controllers for both stator flux and electromagnetic torque, as depicted in Figure 2.

Based on the figure, the reference stator flux Ψ_s* and reference torque T_e* are compared with their respective estimated values. The stator flux and torque errors are processed by hysteresis band comparators. Specifically, the through stator flux is regulated by a two-level hysteresis comparator, while the torque is controlled by a three-level comparator. Based on the outputs of these comparators and the stator flux sector, an appropriate voltage vector for the voltage source inverter (VSI) is selected from the switching table shown in Table 1.

In a symmetrical three-phase induction machine, the instantaneous electromagnetic torque is generally proportional to the cross product of the stator flux space vector and the rotor flux space vector [24].

$$T_e = \left(\frac{3p}{2}\right) \psi_s \psi_r \sin(\delta) \tag{19}$$

Where Ψs: represents the stator flux space vector, Ψr: denotes the rotor flux space vector (referred to the stator), and Δ: is the angle between the stator and rotor flux vectors. The equations used to estimate the stator flux ψ_s, its position θ_s, and the electromagnetic torque are expressed as (20) to (22):

$$\psi_s = \sqrt{{\psi_{qs}}^2 + {\psi_{ds}}^2} \tag{20}$$

$$\theta_s = \tan^{-1}\left(\frac{\psi_{qs}}{\psi_{ds}}\right) \tag{21}$$

$$T_e = \left(\frac{3p}{2}\right)(\psi_{ds} i_{qs} - \psi_{qs} i_{ds}) \quad (22)$$

Table 1. Inverter switching table

Sectors		S1	S2	S3	S4	S5	S6
	dTe = 1	V2	V3	V4	V5	V6	V1
dψs = 0	dTe = 0	V7	V0	V1	V2	V3	V4
	dTe = −1	V6	V1	V2	V3	V4	V5
	dTe = 1	V3	V4	V5	V6	V1	V2
dψs = 1	dTe = 0	V4	V5	V6	V1	V2	V3
	dTe = −1	V5	V6	V1	V2	V3	V4

6. SENSITIVITY ANALYSIS OF IM PARAMETERS

6.1. Overview

Changes in motor parameters can significantly affect the dynamic behavior of drive systems. In the case of indirect field-oriented control (IFOC), performance is influenced by rotor inductance L_r, stator inductance L_s, and rotor resistance R_r. Conversely, for direct torque control (DTC) using a switching table, performance primarily depends on the stator resistance R_s. To quantify these effects, a Jacobian matrix J can be constructed, capturing the sensitivities of torque, speed, and other relevant output variables with respect to variations in motor parameters. For IFOC, the Jacobian matrix typically takes (23):

$$\begin{pmatrix} \Delta T^e \\ \Delta w_{rm} \end{pmatrix} = J_{IFOC} \begin{pmatrix} \Delta L_r \\ \Delta L_s \\ \Delta R_r \end{pmatrix} \quad (23)$$

where:

$$J_{IFOC} = \begin{pmatrix} \frac{\partial T^e}{\partial L_r} & \frac{\partial T^e}{\partial L_s} & \frac{\partial T^e}{\partial R_r} \\ \frac{\partial w_{rm}}{\partial L_r} & \frac{\partial w_{rm}}{\partial L_s} & \frac{\partial w_{rm}}{\partial R_r} \end{pmatrix} \quad (24)$$

For direct torque control (DTC) using a switching table, the Jacobian matrix is simpler and primarily reflects the sensitivity of the system to variations in stator resistance R_s.

$$\begin{pmatrix} \Delta T^e \\ \Delta w_{rm} \end{pmatrix} = J_{DTC-ST}[\Delta R_s \quad (25)$$

Where:

$$J_{DTC-ST} = \begin{pmatrix} \frac{\partial T^e}{\partial R_s} \\ \frac{\partial w_{rm}}{\partial R_s} \end{pmatrix} \quad (26)$$

It is important here to consider the torque and speed ripples under control for both IFOC and DTC. While sensitivity analyses result in steady-state variations of T_e and w_{rm}, dynamic variations may also arise due to the control process itself.

In particular, for a given stator current under hysteresis control, deriving the above Jacobian matrices becomes challenging due to the nonlinear switching dynamics involved. If the stator current is expressed as (27).

$$i_s = I_s + \Delta i_s \quad (27)$$

Where Δi_s represents the hysteresis band width, the expected values of the electromagnetic torque T^e and rotor speed w_{rm} are (28) and (29).

$$T^e = T^e_{(offset)} + \Delta T^e_{(hys)} \quad (28)$$

$$w_{rm} = w_{rm(offset)} + \Delta w_{rm(hys)} \quad (29)$$

Denoting the time average of a variable x by ⟨x⟩, the resulting averages become (30) and (31).

$$\langle T^e \rangle = \langle T^e_{(offset)} \rangle + \langle \Delta T^e_{(hys)} \rangle \quad (30)$$

$$\langle w_{rm} \rangle = \langle w_{rm(offset)} \rangle + \langle \Delta w_{rm(hys)} \rangle \quad (31)$$

No offset occurs if $\langle \Delta T^e_{(hys)} \rangle$and $\langle \Delta w_{rm(hys)} \rangle$ are zero. However, a zero-mean ripple is not guaranteed in general and must be compensated through an integral gain in the control loops. To examine the sensitivities of (24) and (26) from a practical standpoint, simulations of both IFOC and DTC were performed with motor parameters increased by +20% and +40%, in addition to nominal values for the regulators and estimators. The results of these simulations are analyzed in the following section.

6.2. Analysis of simulation results comparing IFOC and DTC

Figures 3 to 6 show the results obtained under parameter variations for both IFOC and DTC. The torque reference is fixed at 20 mN. For IFOC, Figure 3 shows that an incorrect rotor resistance mainly affects the transient behavior, with a 40% increase—possibly due to a broken bar—while the steady-state torque offset remains almost unaffected. Figure 4 indicates that the impact of a stator inductance error is negligible, leading to only a minimal torque deviation. Conversely, Figure 5 shows that a rotor inductance error has a smaller impact, influencing the transient response but leaving the steady state unchanged. Figure 6 indicates that DTC is relatively insensitive to variations of the tested parameter, with minimal impact on both the steady-state torque offset and the dynamic.

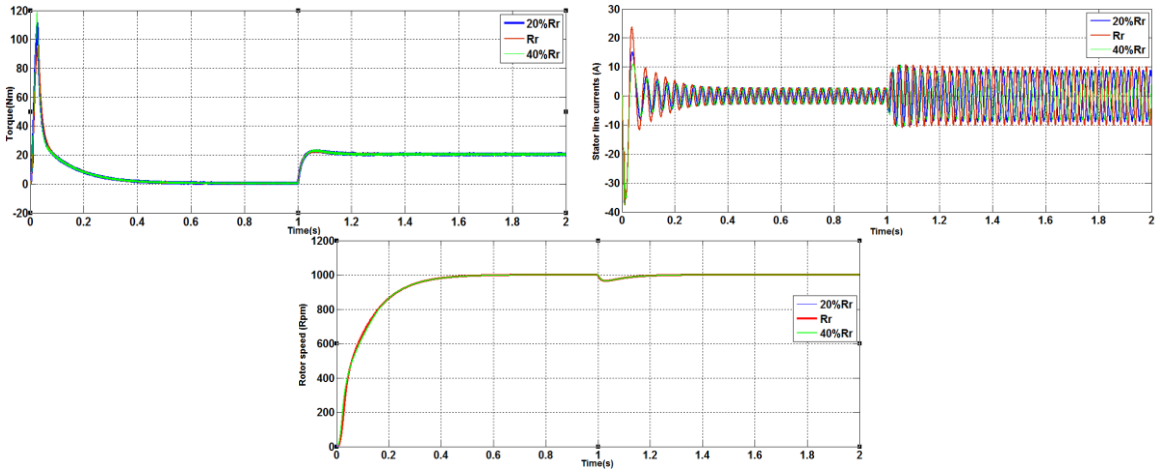

Figure 3. Sensitivity of IFOC to Rr variations

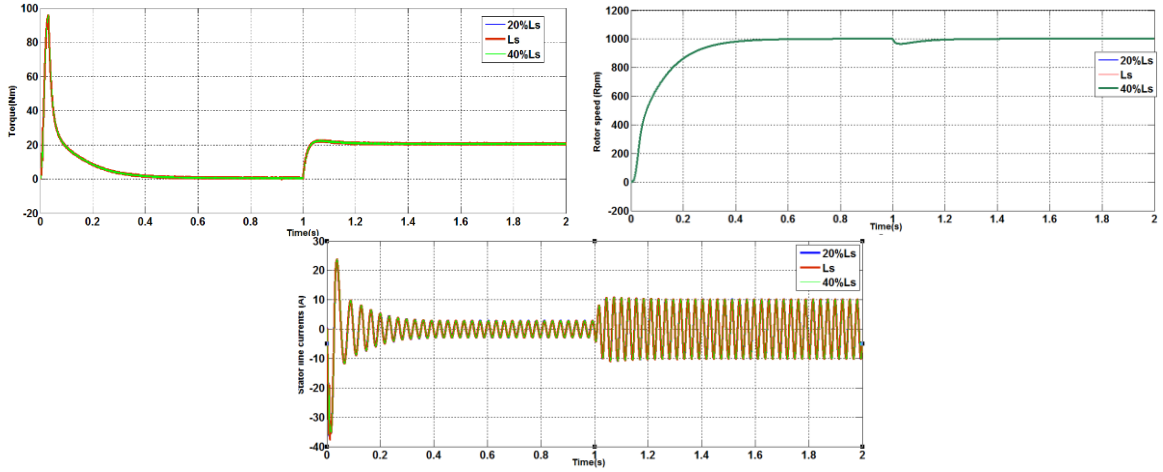

Figure 4. Sensitivity of IFOC to Ls variations

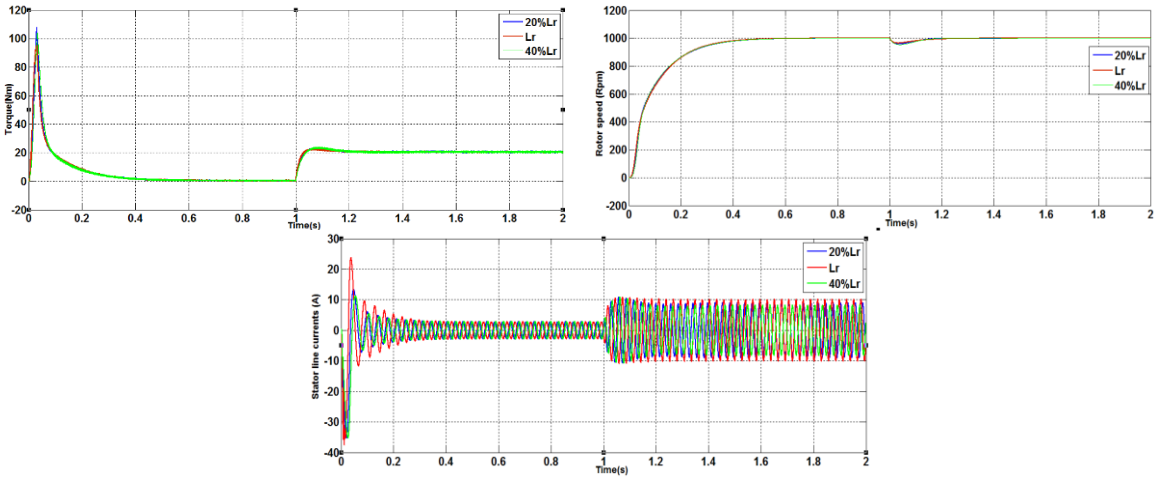

Figure 5. Sensitivity of IFOC to Lr variations

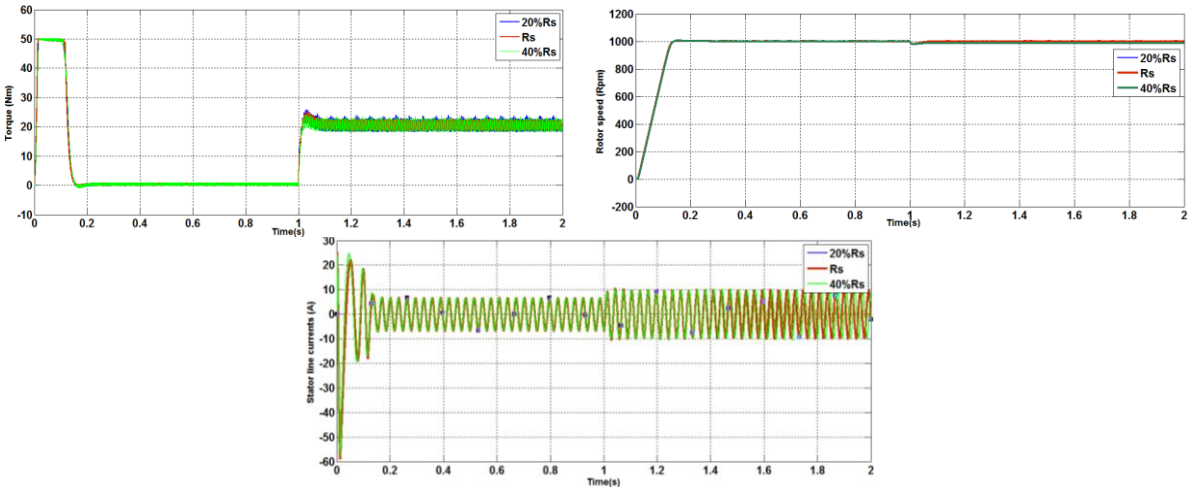

Figure 6. Sensitivity of DTC to Rs variations

7. FLUCTUATING RESPONSES

Both IFOC and DTC serve as torque transducers with strong tracking capabilities. Their dynamic performance is generally compared independently of the specific switching schemes used by each method. To emulate an electric or hybrid vehicle driving cycle, a stepped torque profile was simulated in Simulink under both control strategies.

The IFOC simulation follows the approach in [25], while the DTC simulation is based on [26]. The motor model employed is a 3-kW asynchronous machine. The simulation ran for 8 seconds, with torque commands of 20, 10, 18, and 14 Nm applied every 2 seconds. Fixed flux references were set at 2.25 Wb for DTC and 1 Wb for IFOC. Simulation results are presented in Figures 7 and 8.

Figure 7 shows that, during the test cycle, the main difference between the two methods lies in response time and stabilization under start-up and load changes. IFOC exhibits a slower speed response, whereas DTC reacts more quickly and stabilizes faster in the steady state. Minor disturbances are observed during speed transitions. Figure 8 highlights that IFOC requires about 0.5 s to reach a steady-state torque of 18 Nm, while DTC achieves the same torque in only 0.1 s. Despite this, the overall torque performance is comparable, showing fast response within the considered time frame. Although it is challenging to directly compare the methods due to differing switching schemes, DTC demonstrates superior dynamic performance in this scenario, with a significantly shorter stabilization time compared to IFOC.

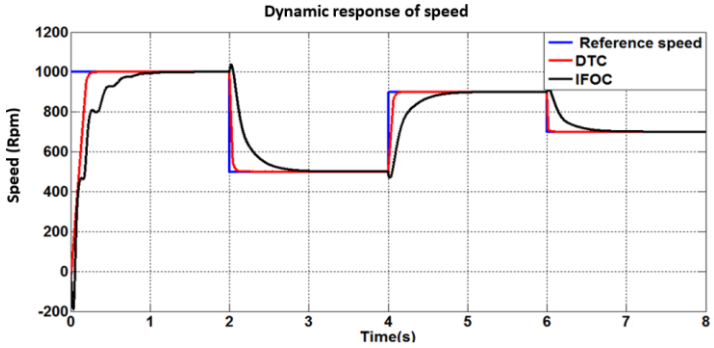

Figure 7. Speed response during a driving cycle

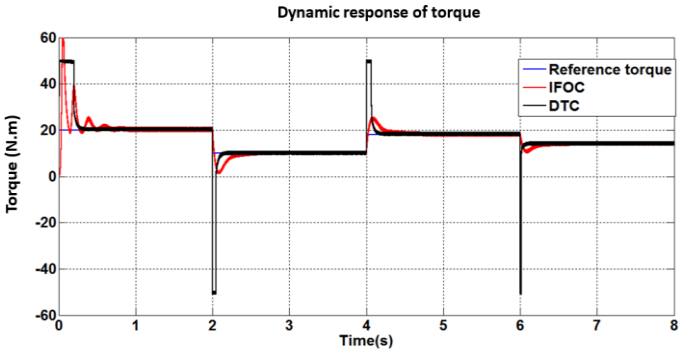

Figure 8. Torque response during a driving cycle

8. EXPERIMENTAL STUDY OF FAULT-TOLERANT DTC AND IFOC CONTROL

In this section, a real-time study is carried out to analyze and compare two fault-tolerant control methods, DTC and IFOC. Both controllers are applied to an induction motor powered by an inverter under fault conditions. The test bench consists of the following components, as shown in Figure 9:

- A PC used for software development and results visualization.
- A dSPACE1104 board connected to the PC and controlled via dedicated software.
- A 3 kW three-phase induction motor with stator windings connected in a delta configuration to a 3×380 V network. The motor parameters are given in Table 2.
- A separately excited generator supplying resistive loads.
- A SEMIKRON power converter consisting of a rectifier and a three-phase inverter.
- Only two current sensors

For DTC, cost can be reduced and hardware minimized by estimating the phase voltages from the DC bus and the inverter switching states (Sa, Sb, Sc), instead of using three voltage sensors. In (32), the estimated phase voltages for DTC are shown in the basic functional diagram in Figure 2.

$$\left.\begin{aligned} V_{an} &= \frac{Vdc}{3}(2S_a - S_b - S_c) \\ V_{bn} &= \frac{Vdc}{3}(-S_a + 2S_b - S_c) \\ V_{cn} &= \frac{Vdc}{3}(-S_a - S_b + 2S_c) \end{aligned}\right\} \quad (32)$$

Figure 10 presents an experimental electrical drive system used for testing a fault-tolerant control strategy based on IFOC–DTC algorithms. The setup includes a network supply feeding the system through an autotransformer, with fault injection capability such as a three-phase break and converter faults. The control architecture is implemented in MATLAB/Simulink and executed via a dSPACE Control Desk platform, which manages the inverter, measurement signals, and real-time control loops.

On the power side, the system drives an induction motor mechanically coupled to a DC generator acting as a resistive load. The measured variables, including stator currents, rotor speed, and electromagnetic torque, are fed back to the control unit for monitoring and adaptation. Isolation and adaptation stages ensure

safe signal conditioning between the power circuit and the control interface, enabling reliable real-time experimentation under both healthy and faulty operating conditions.

Figure 9. Photograph of the experimental test bench

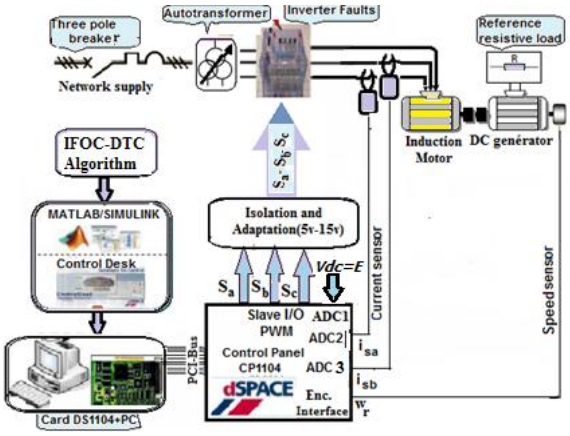

Figure 10. Overview of the experimental electrical drive system

Table 2. 3-kW induction motor parameters

Greatness	Value	Greatness	Value
Nominal compound voltage: U	380 V	Stator leakage inductance: L_s	0.5668 H
Nominal torque: T_n	20 Nm	Rotor leakage Inductance: L_r	0.5142 H
Nominal line current: I_s	7 A	Mutual inductance: M	0.5142 H
Coupling	Δ	Number of pair poles: $2p$	2
Rotor resistance: R_r	2.8 Ω	Moment of intertie: j	0.058 kgm
Stator resistance: R_s	6 Ω	Coefficient of viscous friction: f	0.005 Nm/rad/s

8.1. Fault-tolerant DTC control

Figures 11(a) to 11(c) illustrate the waveforms of the electromagnetic torque, the stator currents (i_{sa}, $i_{s\beta}$, i_sC), and the rotational speed. The results obtained from the DTC under both fault and fault-tolerant modes are displayed on the Control Desk software interface in Figure 12, with the fault introduced at t = 7 s. These results highlight the dynamic behavior of the system during the occurrence of the fault and after the activation of the fault-tolerant strategy. They also show how the control system responds to disturbances in real time. Furthermore, the presented waveforms allow a clear evaluation of the stability and performance of the DTC approach under faulty operating conditions.

8.2. FOC control fault-tolerant

Figures 13(a) to 13(c) show the waveforms of the electromagnetic torque, the stator currents (i_{sa}, $i_{s\beta}$, i_sC), and the rotational speed. The results obtained from IFOC under both fault and fault-tolerant modes are displayed on the Control Desk software interface in Figure 14, with the fault introduced at t = 7 s. These results illustrate the behavior of the system before and after the occurrence of the fault. They provide insight into the capability of the IFOC strategy to maintain acceptable performance under disturbed conditions. Moreover, the waveforms enable a detailed analysis of the dynamic response and the stability of the system during fault conditions.

It can be observed that a single inverter fault causes the electromagnetic torque of the induction motor to increase to 30 mN·m for both DTC and IFOC. DTC produces a noisier torque signal, whereas IFOC maintains a smoother response (Figures 11(a) and 13(a)). At the moment of the fault, the stator current of one phase drops to zero during the positive half-cycle, as shown in Figures 11(b) and 13(b). Figures 11(c) and 13(c) show that the motor speed remains stable in real time under the fault-tolerant condition at t=7 s, following only a slight disturbance for both control strategies. Table 3 presents a comparison between the two controllers. It can be concluded that both proposed and compared control strategies are robust and demonstrate effective fault-tolerant capabilities.

Table 3. Comparison table between DTC and IFOC

Parameter	Direct torque control (DTC)	Indirect field-oriented control (IFOC)
Response time (Speed)	0.9 s	1s
Stability	From 9s under tolerated fault from 4s under load	From 10 s under tolerated fault from 5 s under load
Accuracy	Low steady-state error (accurate)	Low steady-state error
Startup overshoot	4%	5%
Disturbances	7.5% under tolerated fault 10% under load	2.5% under tolerated fault 12.5% under load

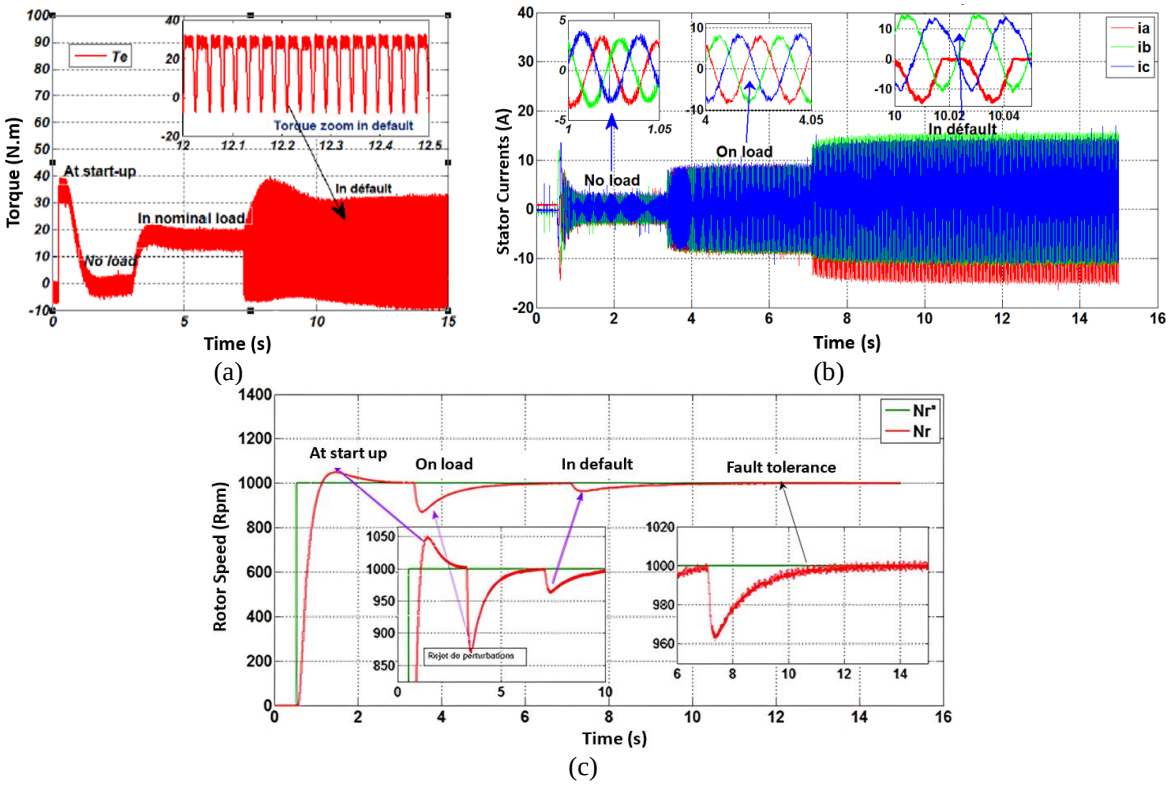

Figure 11. Experimental results of DTC with fault tolerance at 7 s: (a) electromagnetic torque in DTC-(N), (b) stator line currents-In IFOC- (A), and (c) motor speed-In DTC-(Rpm)

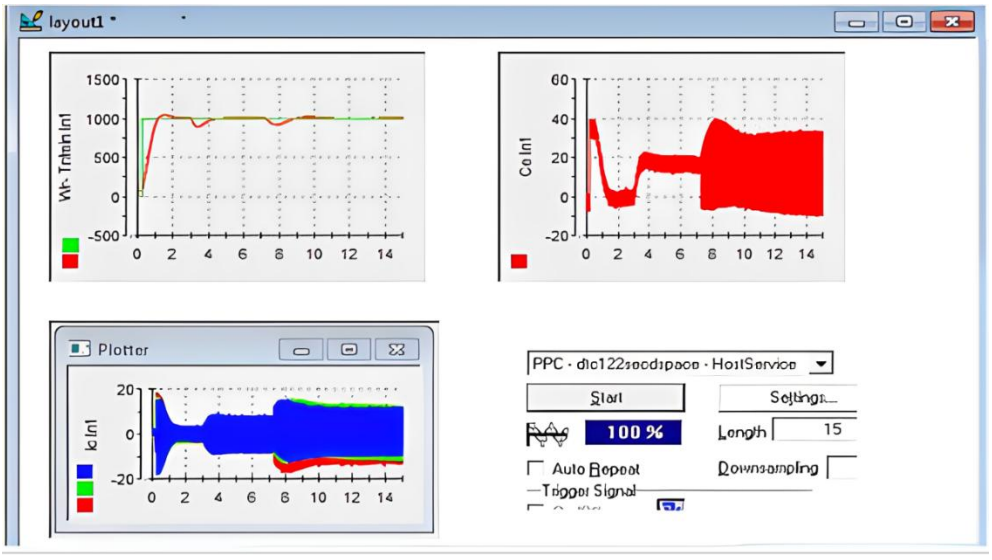

Figure 12. Software interface control panel for DTC in fault tolerance

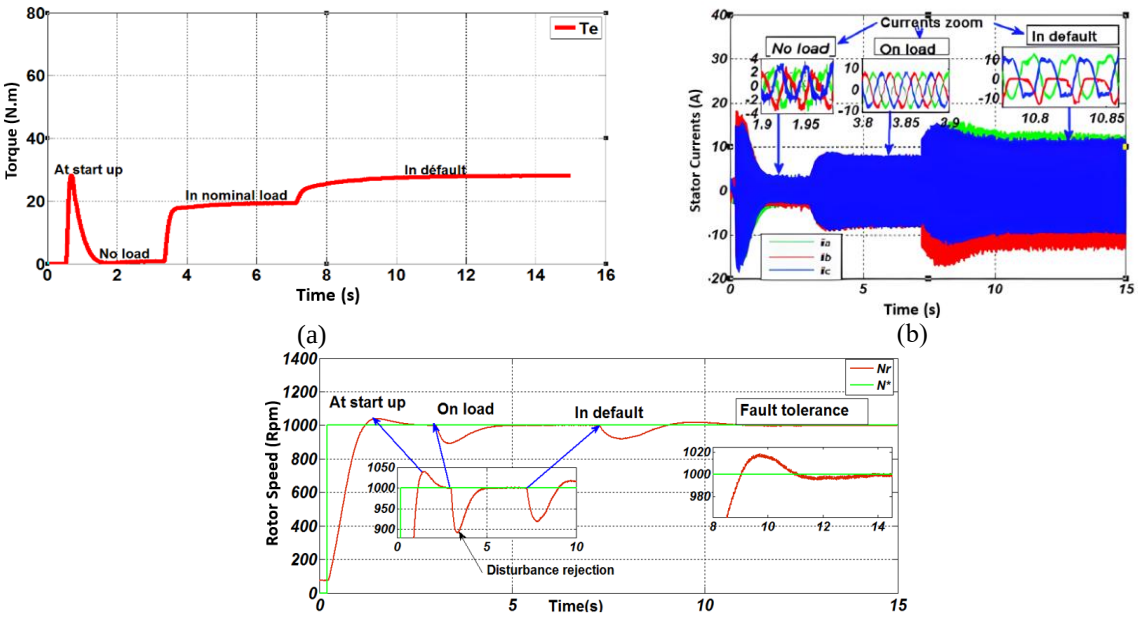

Figure 13. Experimental results of IFOC with fault tolerance at 7 s: (a) electromagnetic torque-in IFOC-(N), (b) stator line currents-in DTC-(A), and (c) rotor speed-in DTC-(Rpm)

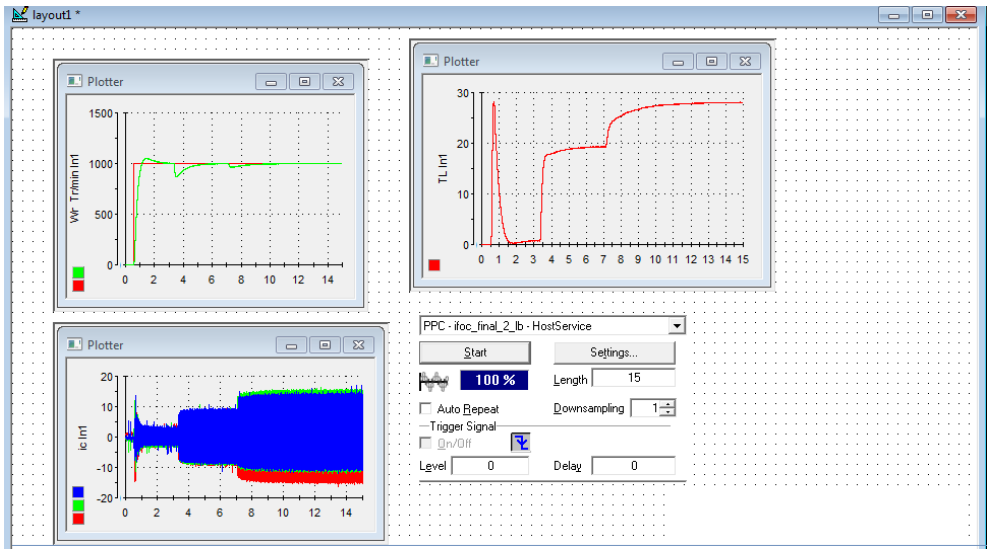

Figure 14. Software interface control panel for IFOC in fault tolerance

9. CONCLUSION

This paper emphasizes that drive control strategies should be analyzed independently of their switching schemes to enable meaningful comparisons of dynamic performance, parameter sensitivity, and behavior under inverter faults. Although debate continues over the most appropriate control approach for applications such as traction, establishing a common comparison framework is essential. Differences in switching schemes between IFOC and DTC can otherwise lead to biased conclusions. When these controls are decoupled from their switching schemes, the distinctions between them become more subtle. In this context, IFOC shows clear advantages in dynamic performance, robustness to parameter variations, and fault tolerance.

At the same time, DTC maintains a significant edge within this same framework, delivering superior transient and steady-state performance, insensitivity to stator resistance, and effective fault tolerance. This underscores the importance of exploring various combinations of drive controls and switching schemes. Future research focusing on identifying the optimal switching scheme for each control type would allow for fairer comparisons and, ultimately, help determine the most efficient motor drive system.

ACKNOWLEDGMENTS

The authors wish to express their deep gratitude to the Algerian Ministry of Higher Education and Scientific Research for its support and encouragement of academic research.

FUNDING INFORMATION

The authors declare that this work was funded by the University of Sciences and Technology M.B. USTO, Algeria.

AUTHOR CONTRIBUTIONS STATEMENT

This journal uses the Contributor Roles Taxonomy (CRediT) to recognize individual author contributions, reduce authorship disputes, and facilitate collaboration.

Name of Author	C	M	So	Va	Fo	I	R	D	O	E	Vi	Su	P	Fu
Asmaa Hammou	✓	✓	✓	✓	✓	✓	✓	✓	✓	✓				
Mokhtar Bendjebbar		✓	✓			✓		✓	✓	✓	✓	✓		
Mohammed Benslimane	✓	✓	✓	✓		✓	✓	✓	✓	✓	✓	✓		

C : **C**onceptualization
M : **M**ethodology
So : **So**ftware
Va : **Va**lidation
Fo : **Fo**rmal analysis
I : **I**nvestigation
R : **R**esources
D : **D**ata Curation
O : Writing - **O**riginal Draft
E : Writing - Review & **E**diting
Vi : **Vi**sualization
Su : **Su**pervision
P : **P**roject administration
Fu : **Fu**nding acquisition

CONFLICT OF INTEREST STATEMENT

The authors declare that they have no conflicts of interest.

DATA AVAILABILITY

Derived data supporting the findings of this study are available from the corresponding author, [MB], on request.

REFERENCES

[1] B. S. S. G. Yelamarthi and S. R. Sandepudi, "Predictive torque control of three-phase induction motor drive with inverter switch fault-tolerance capabilities," *IEEE Journal of Emerging and Selected Topics in Power Electronics*, vol. 9, no. 3, pp. 2774–2788, 2021, doi: 10.1109/JESTPE.2020.3020328.

[2] Z. Q. Zhu and K. D. Hoang, "Comparative performance study of alternate fault-tolerant inverter configurations for direct torque control-based three-phase PM BLAC drives under single-phase open-circuit fault," in *8th IET International Conference on Power Electronics, Machines and Drives (PEMD 2016), Institution of Engineering and Technology*, 2016, pp. 6, doi: 10.1049/cp.2016.0193.

[3] M. A. Fnaiech, F. Betin, G. A. Capolino, and F. Fnaiech, "Fuzzy logic and sliding-mode controls applied to six-phase induction machine with open phases," *IEEE Transactions on Industrial Electronics*, vol. 57, no. 1, 2010,doi: 10.1109/TIE.2009.2034285.

[4] M. Bouakoura, N. Nait-Said, M. S. Nait-Said, and A. Belbach, "Novel speed and current sensor FDI schemes with an improved aftc for induction motor drives," *Advances in Electrical and Electronic Engineering*, vol. 16, no. 1, 2018, doi: 10.15598/aeee.v16i1.2573.

[5] K. Klimkowski and M. Dybkowski, "Adaptive fault-tolerant direct torque control structure of the induction motor drive," in *2015 International Conference on Electrical Drives and Power Electronics, EDPE 2015 - Proceedings, Tatranska Lomnica, Slovakia*, 2015, pp. 7–12. doi: 10.1109/EDPE.2015.7325261.

[6] I. Takahashi and T. Noguchi, "A new quick-response and high-efficiency control strategy of an induction motor," *IEEE Transactions on Industry Applications*, vol. IA-22, no. 5, pp. 820–827, 1986, doi: 10.1109/TIA.1986.4504799.

[7] M. Depenbrock, "Direct self-control (DSC) of inverter-fed induction machine," *IEEE Transactions on Power Electronics*, vol. 3, no. 4, pp. 420–429, 1988, doi: 10.1109/63.17963.

[8] C. A. Martins and A. S. Carvalho, "Technological trends in induction motor electrical drives," in *2001 IEEE Porto Power Tech Proceedings*, 2001, pp. 97–104. doi: 10.1109/PTC.2001.964725.

[9] M. Bermúdez, H. Guzmán, I. González-Prieto, F. Barrero, M. J. Durán, and X. Kestelyn, "Comparative study of DTC and RFOC methods for the open-phase fault operation of a 5-phase induction motor drive," in *IECON 2015 - 41st Annual Conference of the IEEE Industrial Electronics Society*, Yokohama, Japan, 2015, pp. 2702–2707. doi: 10.1109/IECON.2015.7392509.

[10] M. Bermudez, I. Gonzalez-Prieto, F. Barrero, H. Guzman, X. Kestelyn, and M. J. Duran, "An experimental assessment of open-phase fault-tolerant virtual-vector-based direct torque control in five-phase induction motor drives," *IEEE Transactions on Power Electronics*, vol. 33, no. 3, pp. 2774–2784, 2018, doi: 10.1109/TPEL.2017.2711531.

[11] A. M. Bazzi, A. P. Friedl, S. Choi, and P. T. Krein, "Comparison of induction motor drives for electric vehicle applications: dynamic performance and parameter sensitivity analyses," in *2009 IEEE International Electric Machines and Drives Conference, IEMDC '09*, Miami, FL, USA, 2009, pp. 639–646. doi: 10.1109/IEMDC.2009.5075273.

[12] T. A. Wolbank, A. Moucka, and J. L. Machl, "A comparative study of field-oriented and direct-torque control of induction motors reference to shaft-sensorless control at low and zero-speed," in *Proceedings of the IEEE International Symposium on Intelligent Control*, IEEE, pp. 391–396. doi: 10.1109/ISIC.2002.1157795.
[13] B. Saad, C. Salim, and D. E. Khodja, "Application of hyper-fuzzy logic type -2 in field-oriented control of induction motor with broken bars international organization of scientific research international organization of scientific research," IOSR Journal of Engineering (IOSRJEN)vol. 08, no. 5, pp. 1–7, 2018,
[14] N. Djeghali, M. Ghanes, S. Djennoune, and J. P. Barbot, "Sensorless fault tolerant control for induction motors," *International Journal of Control, Automation and Systems*, vol. 11, no. 3, pp. 563–576, 2013, doi: 10.1007/s12555-012-9224-z.
[15] Z. Gao, C. Cecati, and S. X. Ding, "A survey of fault diagnosis and fault-tolerant techniques-part i: fault diagnosis with model-based and signal-based approaches," *IEEE Transactions on Industrial Electronics*, vol. 62, no. 6, 2015, doi: 10.1109/TIE.2015.2417501.
[16] R. Maamouri, M. Trabelsi, M. Boussak, and F. M'Sahli, "Second-order SMO-based sensorless control of IM drive: experimental investigations of observer sensitivity and system reconfiguration in postfault operation mode," *IET Electric Power Applications*, vol. 15, no. 7, pp. 811–823, 2021, doi: 10.1049/elp2.12057.
[17] M. Moujahed, B. Touaiti, H. Benazza, M. Jemli, and M. Boussak, "Extended Kalman filter for sensorless fault tolerant control of pmsm with stator resistance estimation," *International Journal of Power Electronics and Drive Systems*, vol. 9, no. 2, pp. 579–590, 2018, doi: 10.11591/ijpeds.v9.i2.pp579-590.
[18] D. Kastha and B. K. Bose, "Investigation of fault modes of voltage-fed inverter system for induction motor drive," *IEEE Transactions on Industry Applications*, vol. 30, no. 4, pp. 1028–1038, 1994, doi: 10.1109/28.297920.
[19] B. Lu and S. K. Sharma, "A literature review of IGBT fault diagnostic and protection methods for power inverters," *IEEE Transactions on Industry Applications*, vol. 45, no. 5, pp. 1770–1777, 2009, doi: 10.1109/TIA.2009.2027535.
[20] R. Peuget, S. Courtine, and J. P. Rognon, "Fault detection and isolation on a PWM inverter by knowledge-based model," *IEEE Transactions on Industry Applications*, vol. 34, no. 6, pp. 1318–1326, 1998, doi: 10.1109/28.739017.
[21] B. Chikondra, U. R. Muduli, and R. K. Behera, "Open-phase fault-tolerant direct torque control for five-phase three-level NPC VSI fed induction motor drive," in *9th IEEE International Conference on Power Electronics, Drives and Energy Systems, PEDES 2020*, Jaipur, India, 2020, pp. 1–6. doi: 10.1109/PEDES49360.2020.9379786.
[22] S. Ahamad and S. Goel, "Fault-tolerant and performability for safety-critical systems: a study based on interrelation," in *SSRN Electronic Journal*, 2021, pp. 1–4. doi: 10.2139/ssrn.3842659.
[23] T. Roubache, S. Chaouch, and M. S. N. Said, "A fault-tolerant control for induction-motors using sliding mode scheme," in *14th International Conference on Sciences and Techniques of Automatic Control and Computer Engineering, STA 2013*, Sousse, Tunisia, 2013, pp. 231–236. doi: 10.1109/STA.2013.6783136.
[24] M. Benslimane, M. Bendjebar, and D. A. Bouayed, "Fault tolerant control implementation for inverter-fed induction motors: a real-time implementation," *Journal Europeen des Systemes Automatises*, vol. 56, no. 4, pp. 605–614, 2023, doi: 10.18280/jesa.560410.
[25] P. C. Krause, O. Wasynczuk, S. D. Sudhoff, and S. D. Pekarek, *Analysis of electric machinery and drive systems, fourth edition*, 2nd ed. New York, USA: Wiley-IEEE Press, 2025. doi: 10.1002/9781394293896.
[26] Z. Sorchini and P. T. Krein, "Formal derivation of direct torque control for induction machines," *IEEE Transactions on Power Electronics*, vol. 21, no. 5, pp. 1428–1436, 2006, doi: 10.1109/TPEL.2006.882086.

BIOGRAPHIES OF AUTHORS

Asmaa Hammou was born in Oran, Algeria, in 1994. She obtained her LMD bachelor's degree in electrical engineering in 2016 from the University of Science and Technology of Oran, USTO-MB, Algeria. In 2018, she received san LMD Master's degree in Electrical Engineering, specializing in Electrical Machines, from USTO-MB. Since 2018, she has been a Ph.D. student in Electrical Engineering, specializing in Control and Diagnosis of Electrical Drives, at the Department of Electrical Engineering, Faculty of Electrical Engineering, University of Science and Technology of Oran, USTO-MB, Algeria. She can be contacted at email: asmaa.hammou@univ-usto.dz.

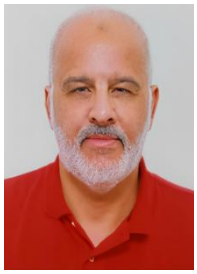

Mokhtar Bendjebbar was born in Relizane, Algeria, on August 16, 1965. He received his engineer, magister, and Ph.D. degrees in Electrical Engineering from the University of Sciences and Technology of Oran Mohamed Boudiaf (USTOMB), Oran, Algeria, in 1989, 1993, and 2006, respectively. He is currently a Professor of Electrical Engineering at USTO-MB. His research interests include electrical machines and drive control, power electronics, and intelligent control. He can be contacted at email: mokhtar.bendjebbar@univ-usto.dz.

Dr. Mohammed Benslimane was born in Oran, Algeria, in 1964. He received his Bachelor's degree from the National Polytechnic School of Oran (ENP-Oran, Algeria) in 1987, his master's degree from the University of Sciences and Technology of Mostaganem, Algeria, in 2013, and his Ph.D. in electrotechnics with a specialization in control and diagnosis of electrical drives from the University of Sciences and Technology of Oran, Algeria, in 2024. Since 2005, he has been working as a training consultant in private schools and state industrial institutions. His research interests include electrical machines, the development of high-performance applications, and the practical implementation of motor drive control systems, along with their associated diagnostics. He can be contacted at email: mohammed.benslimane@univ-usto.dz.